UCRL-17423

cy. 2

University of California

Ernest O. Lawrence Radiation Laboratory

THE MORPHOLOGY OF THE FIELD ION SPECIMEN

RECEIVED
LAWRENCE
RADIATION LABORATORY
JUL 14 1967
LIBRARY AND
DOCUMENTS SECTION

TWO-WEEK LOAN COPY

This is a Library Circulating Copy which may be borrowed for two weeks. For a personal retention copy, call Tech. Info. Division, Ext. 5545

Berkeley, California

DISCLAIMER

This document was prepared as an account of work sponsored by the United States Government. While this document is believed to contain correct information, neither the United States Government nor any agency thereof, nor the Regents of the University of California, nor any of their employees, makes any warranty, express or implied, or assumes any legal responsibility for the accuracy, completeness, or usefulness of any information, apparatus, product, or process disclosed, or represents that its use would not infringe privately owned rights. Reference herein to any specific commercial product, process, or service by its trade name, trademark, manufacturer, or otherwise, does not necessarily constitute or imply its endorsement, recommendation, or favoring by the United States Government or any agency thereof, or the Regents of the University of California. The views and opinions of authors expressed herein do not necessarily state or reflect those of the United States Government or any agency thereof or the Regents of the University of California.

Submitted to
Journal of Applied Physics

UCRL-17423
PREPRINT

UNIVERSITY OF CALIFORNIA
Lawrence Radiation Laboratory
Berkeley, California

Contract No. W-7405-eng-48

THE MORPHOLOGY OF THE FIELD ION SPECIMEN

S. Ranganathan, H. B. Lyon
and G. Thomas

March 1967

THE MORPHOLOGY OF THE FIELD ION SPECIMEN

S. Ranganathan, H. B. Lyon and G. Thomas

Inorganic Materials Research Division, Lawrence Radiation Laboratory,
and Department of Mineral Technology, College of Engineering,
University of California, Berkeley, California

ABSTRACT

The simulation of field ion images by computation of the position of atoms which lie within an outer shell of given thickness on a spherical crystal has been extended to spherical crystals of a variety of structures. These include the hexagonal lattice, the hexagonal close-packed structure and a few of the common superlattices. The consequences of the invisibility of one atomic species in ordered alloys has been investigated. The results show that computations are in fact necessary for a detailed interpretation of the field ion image.

1. INTRODUCTION

In crystal growth the structure of the crystal is known to play an important part in the morphology of the crystal. In fact before the advent of x-rays the morphology was often used to make valuable deductions concerning the structure of the material. Bravais[1] was the first to recognize that the interplanar distance determines whether a particular face appears in the resultant crystal or not. Donnay and Harker[2] gave this idea a precise formulation. They took lattice centering, screw axes and glide planes into account and used the multiple indices of the lowest order of x-ray reflection in computing interplanar distances.

The latter consideration is applicable to the field ion specimen as well and enables us to list the planes for a given lattice in terms of decreasing interplanar distance. Such a list gives the morphological importance of the planes. The size and the number of $(hk\ell)$ rings on a field ion image is a measure of the importance of the $(hk\ell)$ plane. Also the list gives the order in which planes develop as the size of the crystal is increased. Drachsler and Wolf[3] were the first to point out the usefulness of x-ray extinction rules in the context of field ion microscopy.

A different approach to the morphology of the field ion specimen was suggested by Moore.[4] Since the image is made up of protruding atoms on the surface of a nearly hemispherical crystal, Moore provided a definition for this protrusion, namely that only those atoms which lie within an outer shell of given thickness can give rise to spots on the image. A computer was used to find out the coordinates of the

atoms within the shell. Recently the Moore model was extended to spheres of varying radii by Moore and Ranganathan.[5] They found that the decreasing interplanar distance rule is nearly exact for any given zone but it cannot be applied to the image as a whole, because there is interference between rings. Also even when a plane is present in the image, it may escape recognition. Moore and Ranganathan also obtained a visibility criterion that requires the presence of at least three atom rows parallel to the dense direction in the plane. This criterion can explain the different rates of development of different zones.

In crystal structures where atoms occupy crystallographically non-equivalent positions the criterion of interplanar distance and inter-row distances cannot be used. Crystals with h.c.p. structures are an example. In such cases simulation of the field ion image by computation is desirable for purposes of comparison, and image interpretation. The situation is analogous to the facility of interpretation of orientations in electron micrographs by means of Kikuchi diffraction maps.[6,7]

Advances in the technique fo field ion microscopy have made it possible to obtain regular images from a number of ordered alloys and intermetallic compounds. In some instances it has been shown that one species of atoms may remain invisible. Computer studies are helpful in checking such possibilities. They can further be used for indexing and detecting anomalous behavior, for example, partial visibility in certain areas. Hence it was thought worthwhile to extend the model of Moore to some of the common superlattices.

This paper thus describes the results of computer calculated images for various crystal structures.

2. METHOD OF CALCULATION

Moore determined the distance of the atom from the spherical envelope. If it were below a set value, p, the coordinates of the atom were recorded. p represents the maximum depth below the spherical surface at which atoms can still contribute to the image. He thus obtained the orthographic projection for b.c.c. and f.c.c. lattice. We have followed a different procedure, but wish to emphasize that the results are identical.

Our method is applicable to any crystal system where two of the axial angles are equal to 90 deg. Only the trigonal and the triclinic systems are excluded. A given crystal structure is considered in terms of the Bravais lattice. If the latter has centering, then the structure can be generated by repeated application of the method to the simple lattice with different coordinates for the origin. Thus, for example, the f.c.c. lattice can be considered to consist of four interpenetrating cubic lattices with origins at (0,0,0), $(\frac{1}{2},\frac{1}{2},0)$, $(0,\frac{1}{2},\frac{1}{2})$, $(\frac{1}{2},0,\frac{1}{2})$. For the simple lattice all atoms are projected onto the basal plane $(hk\ell)$. Then the annuli formed by the intersection of the spherical shell with $(hk\ell)$ planes are also projected onto the basal plane. The atoms in the basal plane are then scanned. The distance of each atom from the center is computed. The coordinates of the atom are recorded if its distance from the center falls within the radius limits of any annulus. The coordinates are then converted to correspond to any desired projection. We have used the stereographic

projection which is a good approximation to the field ion image. The Calcomp plotter subroutine was used to plot the simulated image. The scanning process was extremely rapid. The calculations were programmed in Fortran for a Control Data 6600 Computer.

3. RESULTS

3-1. H.C.P. Metals

Figures 1 and 2 show the computed images for h.c.p. metals with axial ratios c/a equal to 1.62 and 1.58. These two values were chosen as they are the pertinent values for rhenium and ruthenium. Melmed[8] has carried out a systematic field ion microscope study of these two metals. The computed images correspond to a radius of 132 c. The value of p was chosen to be 0.05a and is near the value Moore and Ranganathan[5] used for a f.c.c. metal of comparable radius. There is very little difference between Figure 1 and Figure 2 in terms of the appearance, size and number of planes. It can be concluded the axial ratio does not play too great a role in determining the appearance of the image. This supports a similar conclusion reached by Hren, quoted in Melmed's paper.[6]

The hexagonal close packed structure consists of two classes of atoms which can be designated as P_0 and P_1 atoms. Even though all the atoms in the h.c.p. structure are chemically alike, they can be divided into these two classes by considering their crystallographic environments. Further, if $(2h + 4k + 3\ell)$ is a multiple of 6, each $(hki\ell)$ plane contains both P_0 and P_1 type atoms. If $(2h + 4k + 3\ell) = 6N \pm \epsilon$ with N an integer and $\epsilon = 1,2,3$, then the $(hk\ell)$ planes through

P_1 atoms lie between the planes through P_0 atoms. The interplanar distance alternates as $(\frac{\epsilon}{6} d_{hk\ell})$, $(d_{hk\ell} - \frac{\epsilon}{6} d_{hk\ell})$.[9] Thus there are four kinds of $(hki\ell)$ surfaces. In x-ray diffraction they can be distinguished by their different intensities as shown in Table I.

Melmed has shown that in rhenium, over most of the image, image points arise from only one class of atom (say P_0). P_1 atoms are either invisible or have been evaporated preferentially. Thus effectively the rhenium image can be simulated by computing the pattern from the hexagonal lattice. To make comparisons, computations were carried out on the assumption that every other basal plane was contributing to the image. Figures 3 and 4 show the results for the values of the axial ratios quoted above. It can be seen that there is a drastic change in the observed number of planes between the pattern from the h.c.p. structure and the pattern from the hexagonal lattice.

Computations were carried out for the hexagonal lattice and the h.c.p. structure with the c/a value equal to 1.58. Results were obtained for radius values of 44, 88 and 132 c. Table II lists the planes that appear in different zones. The p value was set at 0.09a for R/c = 44 and at 0.07a for R/c = 88, where R is the radius of the spherical crystal. This has been done as Moore and Ranganathan[5] found that the thickness of the shell has to be increased when the crystal is smaller in size, if there is to be correspondence with the number of image points in experimental images.

Table II lists the planes that are observed along three important zones in the computed pattern for both the hexagonal lattice and the h.c.p. structure. The hexagonal lattice is a Bravais lattice. For

Table I. Characteristics of Planes in H.C.P. Crystals

Type	$2h + 4k + 3\ell$	Examples	x-Ray Intensity	Appearance in Computed Patterns Compared to Hexagonal Lattice
I	$6N$	$11\bar{2}0$, $11\bar{2}2$ $41\bar{5}0$, $30\bar{3}2$	$4f^2$	Enhanced importance
II	$6N \pm 1$	$10\bar{1}1$, $10\bar{1}3$ $20\bar{2}1$, $40\bar{4}1$	$3f^2$	About the same importance
III	$6N \pm 2$	$10\bar{1}0$, $10\bar{1}2$ $21\bar{3}0$, $31\bar{4}0$	f^2	About the same importance
IV	$6N \pm 3$	0001, $11\bar{2}1$ $30\bar{3}1$	0	Reduced importance

Table II. Appearance of Planes in Hexagonal and H.C.P. Patterns

Zones		$10\bar{1}0$-$11\bar{2}0$		0001-$10\bar{1}0$		0001-$11\bar{2}0$	
		hex.	h.c.p.	hex.	h.c.p.	hex.	h.c.p.
Expected planes for various THP radii (R/C)	44	$10\bar{1}0$ $11\bar{2}0$	$10\bar{1}0$ $11\bar{2}0$	0001 $10\bar{1}0$ $10\bar{1}1$ $10\bar{1}2$	0002 $10\bar{1}0$ $10\bar{1}1$ $10\bar{1}2$	0001 $11\bar{2}0$ $11\bar{2}1$ $11\bar{2}2$	0002 $11\bar{2}0$ $11\bar{2}2$ $11\bar{2}4$
	88	$21\bar{3}0$	$41\bar{5}0$ $21\bar{3}0$	$10\bar{1}3$ $20\bar{2}1$ $10\bar{1}4$ $20\bar{2}3$	$10\bar{1}3$ $20\bar{2}1$	$11\bar{2}3$ $11\bar{2}4$	$22\bar{4}2$ $11\bar{2}6$ $11\bar{2}8$ $22\bar{2}6$
	132	$31\bar{4}0$	$31\bar{4}0$	$10\bar{1}5$ $30\bar{3}1$ $30\bar{3}2$ $20\bar{2}5$	$10\bar{1}4$ $10\bar{1}5$ $20\bar{2}3$ $20\bar{2}5$ $50\bar{5}2$ $40\bar{4}1$	$11\bar{2}5$ $22\bar{4}1$ $11\bar{2}6$ $11\bar{2}7$	$33\bar{6}2$ $33\bar{6}4$ $11\ \bar{2}\ 10$

any given zone the planes are expected to appear in the order of decreasing interplanar distance. This is found to be the case. The decreasing interplanar distance corresponds to increasing mesh size of the surface plane. The square of the mesh size is given by $0.75a^2c^2\{1.33(h^2 + hk + k^2) + 0.4\ell^2\}$ for the c/a value of 1.58. The planes appear in different zones in the order determined by this quantity.

A similar straightforward correlation with the interplanar distance is not to be expected in the h.c.p. structure as the interplanar distance is not single valved for a number of $(hki\ell)$ planes. Table I gives the predicted differences in patterns from the h.c.p. structure on the assumption that when $\epsilon = 3$, $(hki\ell)$ should be quoted as $(\underset{\sim}{o}h, \underset{\sim}{o}k, \underset{\sim}{o}i, \underset{\sim}{o}\ell)$ where $\underset{\sim}{o} = 2$, as the interplanar distance is halved. For ϵ values of 1 and 2, $(hki\ell)$ planes can be indexed as $(hki\ell)_B$ to correspond to the P_0 and P_1 surfaces. These considerations can be used to explain the differences between the two patterns. It must be emphasized that computed patterns are necessary as the degree of dominance and reduction in importance for various planes are not easily evoluated by other means.

In the [0001] zone in h.c.p., $(41\bar{5}0)$ gains prominence over $(21\bar{3}0)$ and $(31\bar{4}0)$ as the former belongs to faces of Type I while the latter two belong to Type III. Also the [0001] zone appears better developed for the h.c.p. structure than for the hexagonal lattice. This is in agreement with the experimental observation of Melmed that the [0001] zone shows the development of more planes for ruthenium than for rhenium.

In the $[11\bar{2}0]$ zones both the hexagonal and h.c.p. patterns show very nearly the same degree of development. Almost all planes in this zone belong to Type II or III. For example $(10\bar{1}1)$ has an alternating interplanar distance of $\frac{1}{6}$ d, $\frac{5}{6}$ d ; $\frac{1}{6}$ d, $\frac{5}{6}$; . . . The two topmost planes have very nearly the same radii and can be mistaken to be a single plane. $(30\bar{3}2)$ is a Type I plane to occur in this zone and shows dominance in the h.c.p. pattern. Also $(30\bar{3}1)$ is a Type IV plane and hence its indices are $(60\bar{6}2)$. It is seen to be suppressed and $(40\bar{4}1)$ precedes this plane in order of appearance.

It is in the $[10\bar{1}0]$ zone that the hexagonal and h.c.p. patterns show marked differences. All the planes in the zone have an ϵ value of 0 or 3. Planes with an ϵ value of 0 are very dominant.

In electron diffraction patterns, the phenomenon of double diffraction leads to the observation of (0001) from a combination of $(0\bar{1}10)$ and $(01\bar{1}1)$, even though (0001) is forbidden as it has a zero value for structure factor. There is no useful analogue in field ion microscopy for this phenomenon.

3-2. Superlattices

Images have been obtained from the σ phase in the W-Re system, cementite, NiBe, $MoNi_4$ and CoPt. Comparisons with computed images can be valuable in establishing the nature of the visible species in these cases. The work of Southworth and Ralph[10] and Tsong and Muller[11] have helped establish that effectively only platinum atoms are being imaged from CoPt in the ordered state. Hren and Newman[12] have obtained images from $MoNi_4$ and found the authors' suggestion that only molybdenum atoms are being imaged to be correct. In this section we report results on B2, $L1_0$ and $L1_2$ type superlattices. For a detailed description of the

geometry of these structures, the review by Marcinkowski[13] may be consulted. This choice was made as they are common superlattices and also as they can be generated by successive combinations of cubic lattices with origins at (0,0,0), ($\frac{1}{2}$,$\frac{1}{2}$,0), and (0,$\frac{1}{2}$,$\frac{1}{2}$). Further combinations with ($\frac{1}{2}$,0,$\frac{1}{2}$) yield the f.c.c. pattern. Figures 5,6,7 and 8 show the results thus obtained, from a single program. The radius is 200a where "a" is the parameter of the unit cell. The p value was set at 0.05a. For the B_2, $L1_0$ and $L1_2$ structures, it is probable that a higher value of p should be used. An independent investigation of Ni_4Mo has shown that the p value increases when one of the species is invisible. However, Moore and Ranganathan[5] have demonstrated that a higher p value merely leads to an increase in the number of visible atoms. It does not lead to an increase in the number of planes. Hence we have used a single p value, since we are mainly interested in the morphological aspects of the image.

A superlattice of the B2 type has the composition AB and its structure is the cesium chloride structure. The A atoms occupy a simple cubic lattice and Fig. 5 shows the type of pattern to be expected from A atoms alone. Polonium is the only metal with the simple cubic lattice as its crystal structure and is an unlikely candidate for field ion microscopic examination. However, NiBe has the cesium chloride structure. McLane[14] has obtained patterns from this compound. The images show that the cube ({001}) planes are more prominent than the dodecahedral ({110}) plane. Hence we can infer that only nickel atoms are being imaged. Figure 9 gives the entire stereogram for the simple cubic lattice. This was obtained by photographic reproduction of the 45° sector.

A superlattice of the $L1_0$ type also has the composition AB. Its structure can be visualized to arise from the f.c.c. lattice by population

of alternate (002) planes with one kind of atom. Figure 6 shows the pattern when only A atoms are being imaged. CoPtI has the $L1_0$ structure. Comparisons with micrographs published by Tsong and Muller[11] show very good correlation. In analyzing the images from CoPtI, Moore and Ranganathan[5] followed a simple approach and stated that fewer planes will appear in the CoPt image, if only platinum atoms are imaged. It can be shown that if mesh size is the criterion for visibility as has been assumed by Drechsler and Wolf,[3] then only planes up to $(h^2 + k^2 + \ell^2)/4$ will appear in the image from CoPt, if planes up to $h^2 + k^2 + \ell^2$ appear for Pt when the crystals are of the same radii. However, this will be true only if all the atoms on the surface are imaged and if there is no interference between various rings. Comparison of Figs. 6 and 9 shows that the reduction in the number of planes is not very much. This is partly because the recognition of planes with very high indices is difficult. An interesting result is that some zones are not affected in terms of the number of visible planes. 111-020 zone is an example.

Planes which are occupied by only one kind of atom can be defined as superlattice planes. The geometrical structure factor rule is that h and k should have the same parity and ℓ the opposite parity. Superlattice planes are prominent in the image if one of the species is invisible. Thus in the 002-020 zone for f.c.c. the order of prominence is {(002, (020)}, (022), {(024), (042)}, while for the $L1_0$ structure the order is (001), (020), (021), (022), (023).

A superlattice of the $L1_2$ type has the composition A_3B. The B atoms occupy the corner sites of the f.c.c. lattice. If they are the only visible atoms, then the pattern will be similar to Fig. 5. A atoms alone will form the pattern in Fig. 7. The pattern is similar to that from the f.c.c.

lattice. However, the motif of atoms on individual planes is different and can be used for finding out whether A atoms alone are visible. Once again superlattice planes will show an alternation in the density of the A atoms. The geometrical structure factor rule is that for superlattice planes $hk\ell$ have mixed purity. Thus (001), (010) are superlattice planes.

Computations can be useful in visualizing patterns from more complicated structures as well. The rapidity of the method is very helpful. Figure 10 shows the pattern to be expected from CoPt II which has an orthorhombic structure. The crystallographic unit cell may be conceived to arise from stacking ten CoPt I tetragonal cells aligned in the [010] direction and switching the content of (001) planes from all platinum atoms to all cobalt atoms halfway along the new cell. This gives rise to an antiphase boundary halfway along the long cell and at subsequent similar intervals along the [010] direction. In Fig. 10 there are forty such antiphase boundaries on (010) planes and arranged in a periodic fashion. The order of importance of planes is not disturbed and is seen to be similar to that of CoPt I (Fig. 6). It is also seen that only superlattice planes show contrast for the antiphase boundary. This is to be expected on the $\bar{g} \cdot \bar{R}$ criterion familiar to electron microscopists. $\bar{g}$ is the reciprocal lattice vector for the plane and $\bar{R}$ is the displacement vector for the antiphase boundary and has a value of $\frac{1}{2}(\bar{1}01)$ for the boundary in Fig. 10. $\bar{g} \cdot \bar{R}$ has nonintegral values for superlattice planes and hence the antiphase boundaries can be seen as a mismatch surface where it crosses these planes. This is yet another area where computed patterns are helpful. Recently Sanwald et al.[15] have been able to confirm the contrast to be expected from dislocations in spherical crystals by simulating the field ion image.

CONCLUSIONS

(1) The interpretation of field ion micrographs is greatly simplified by the use of computed patterns particularly in crystal structures of lower symmetry than the cubic systems.

(2) Computations are necessary and valuable in cases where a single criterion such as interplanar distance cannot be applied.

(3) The patterns from hexagonal and h.c.p. crystals and several common superlattices have been computed and the factors that influence the appearance of these images have been discussed.

(4) The contrast from antiphase boundaries has been simulated and is in agreement with theoretical considerations.

ACKNOWLEDGEMENTS

This paper was stimulated by the discussions one of the authors had with Dr. A. J. W. Moore. We are grateful to Mr. W. Dempster of the Computer Center for assistance with the programming. The continued financial support of the United States Atomic Energy Commission is gratefully appreciated.

REFERENCES

1. M. A. Bravais, J. École Polytech. (Paris), Cahier 33, Tome XIX, 1850.
2. J. D. H. Donnay and D. Harker, Am. Mineralogist, 22, 446 (1937).
3. M. Drechsler and P. Wolf, 4th International Conference for Electron Microscopy (Berlin, Springer, 1958), p. 835.
4. A. J. W. Moore, J. Phys. Chem. Solids, 23, 907 (1962).
5. A. J. W. Moore and S. Ranganathan, Phil. Mag., submitted for publication, 1967.
6. E. Levine, W. L. Bell and G. Thomas, J. Appl. Phys. 37, 2141 (1966).
7. P. R. Okamoto, E. Levine and G. Thomas, J. Appl. Phys. (in press).
8. A. J. Melmed, Surface Science, 5, 359 (1966).
9. J. F. Nicholas, An Atlas of Crystal Surfaces, (Gordon and Breach, New York, 1965).
10. H. N. Southworth and B. Ralph, Phil. Mag. 14, 383 (1966).
11. T. T. Tsong and E. W. Müller, Appl. Phys. Letters 9, 7 (1966).
12. R. Newman and J. J. Hren, Private Communication, 1966.
13. M. J. Marcinkowski, Electron Microscopy and the Strength of Crystals, (Interscience Publishers, New York, 1963), p. 333.
14. B. McLane, Thesis, Pennsylvania State University, 1965.
15. R. C. Sanwald, S. Ranganthan and J. Hren, Appl. Phys. Letters 9, 393 (1966).

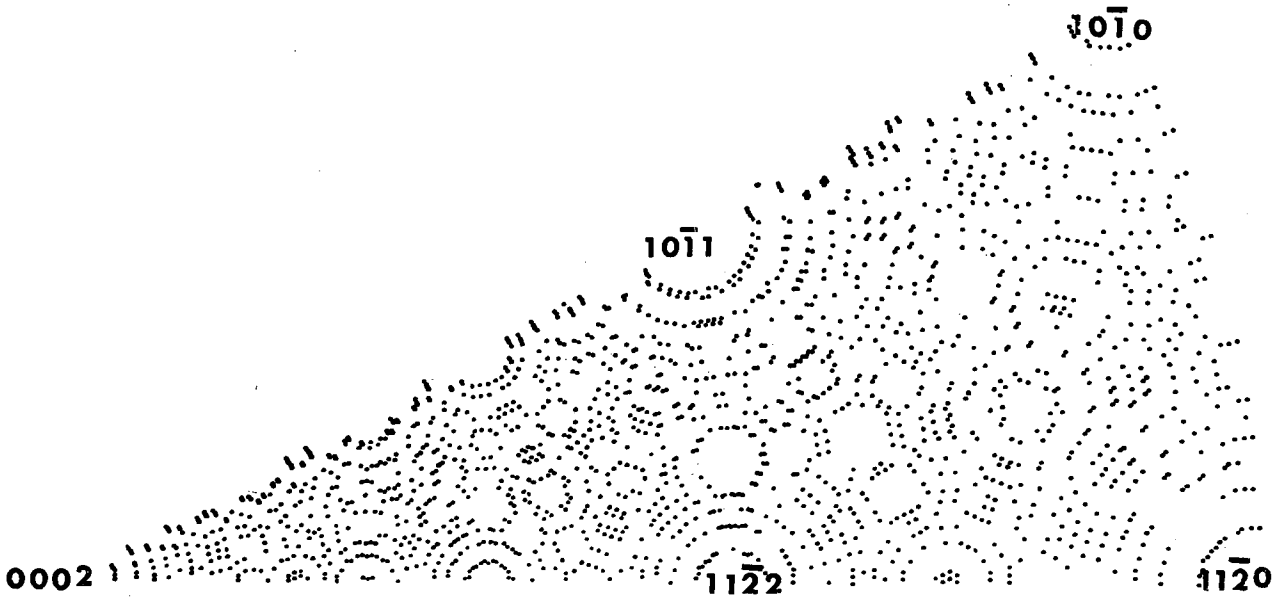

XBL 674-1418

Fig. 1 Computed pattern for spherical surface of h.c.p. structure. c/a = 1.62; R/c = 132.

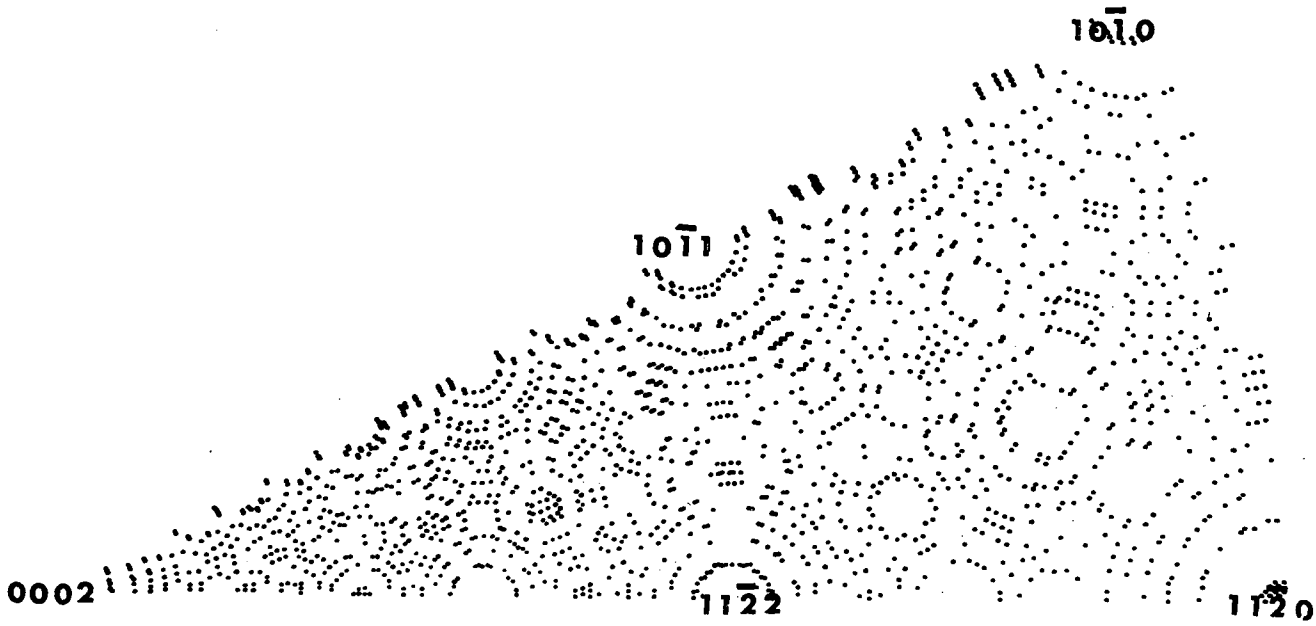

XBL 674-1419

Fig. 2 Computed pattern for spherical surface of h.c.p. structure. c/a = 1.58; R/c = 132.

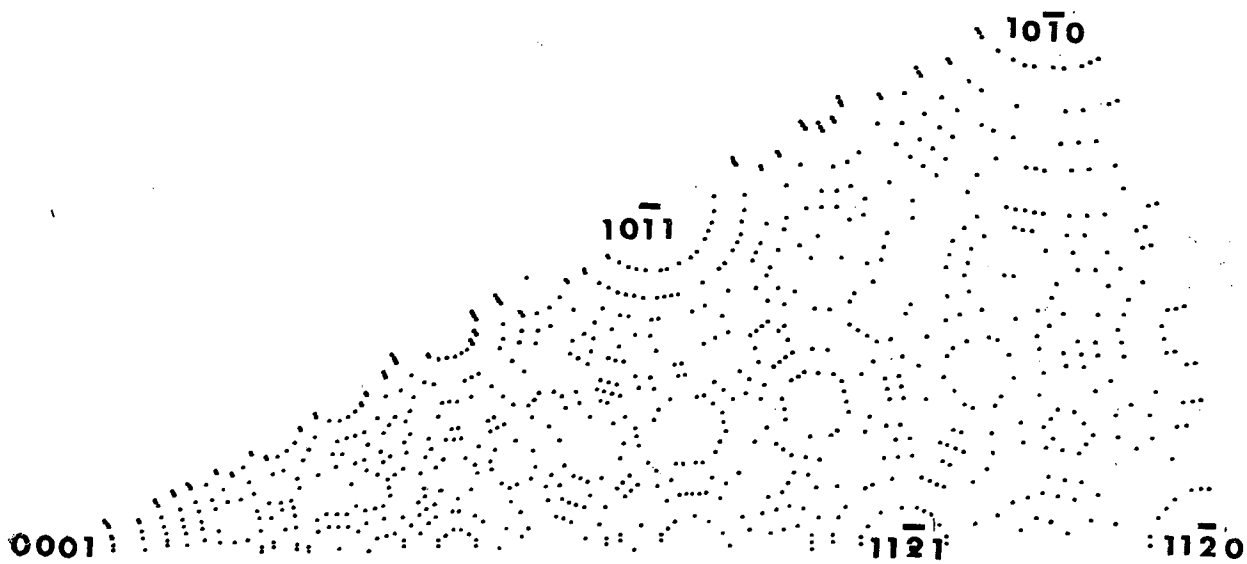

XBL 674-1420

Fig. 3 Computed pattern for spherical surface of hexagonal lattice. c/a = 1.62; R/c = 132.

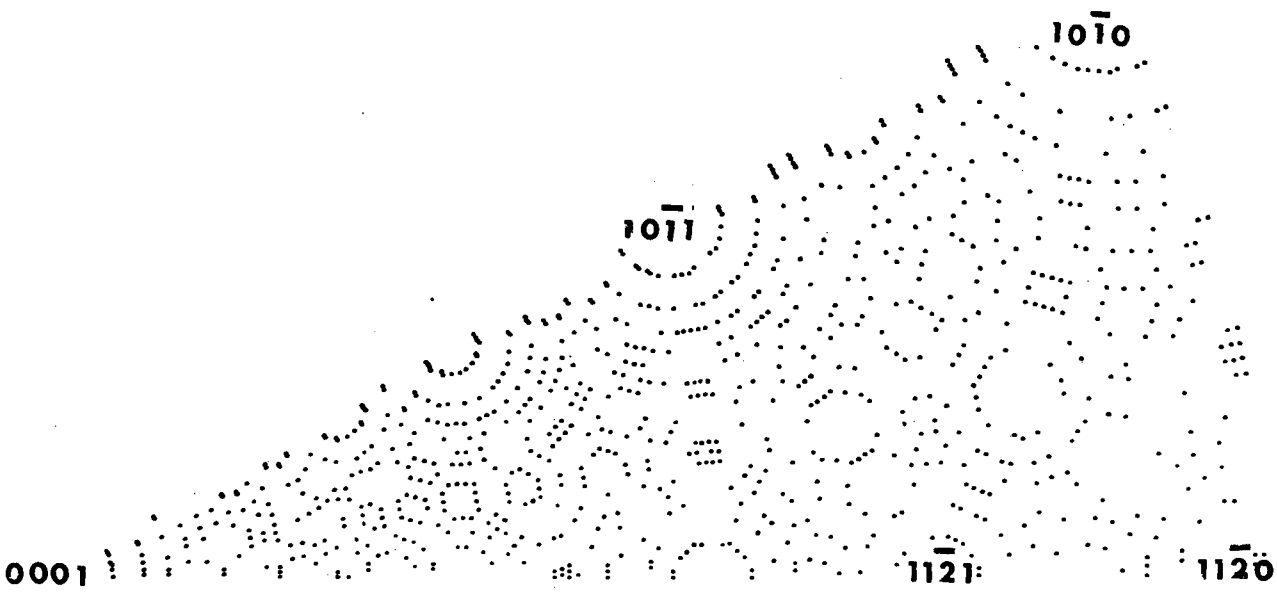

XBL 674-1421

Fig. 4 Computed pattern for spherical surface of hexagonal lattice. c/a = 1.58; R/c = 132.

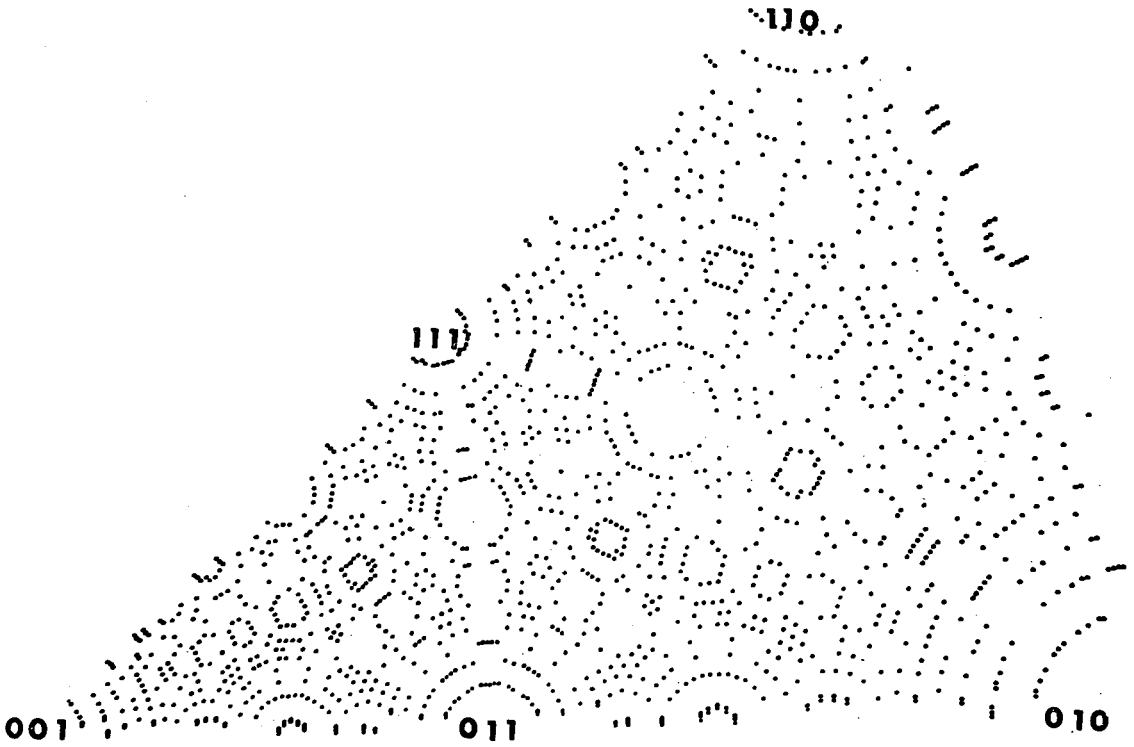

XBL 674-1422

Fig. 5 Computed pattern for the simple cubic lattice; also for the B2 type superlattice with B atoms being invisible.

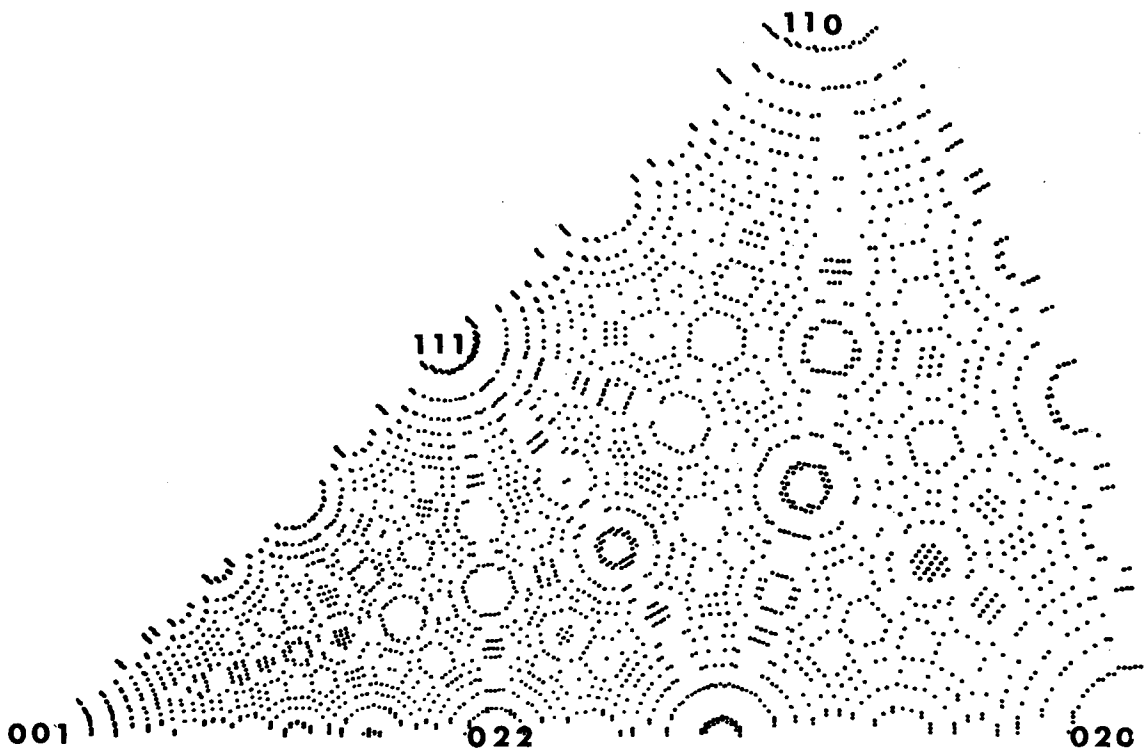

XBL 674-1423

Fig. 6 Computed pattern for the $L1_0$ type superlattice with B atoms invisible.

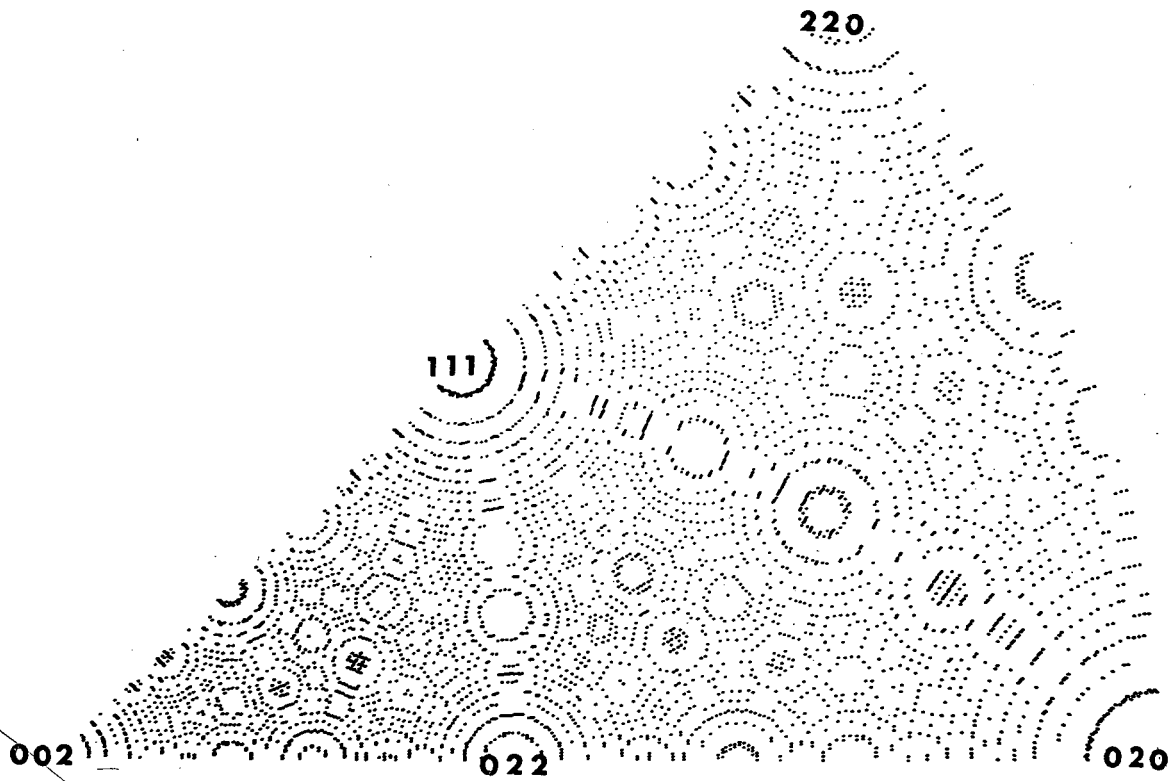

XBL 674-1424

Fig. 7 Computed pattern for $L1_2$ type superlattice with B atoms invisible.

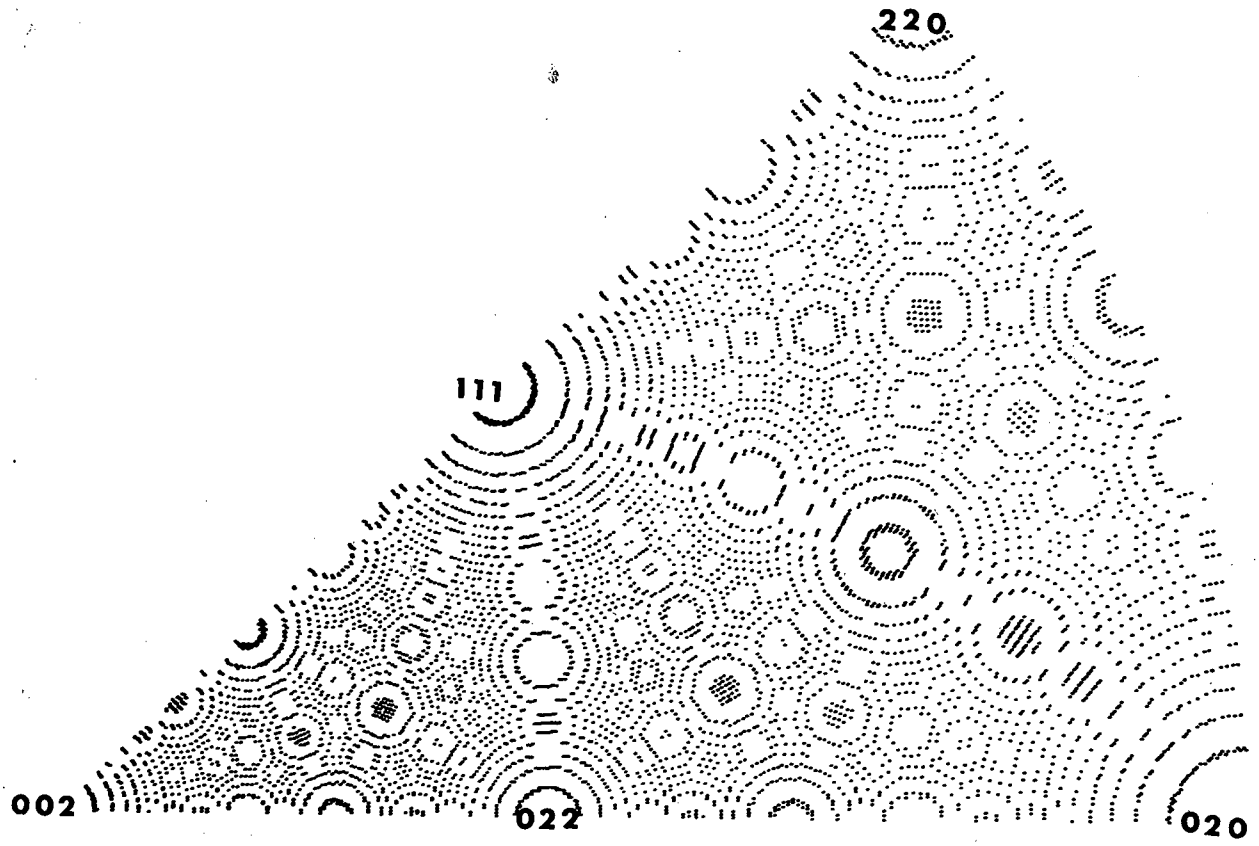

XBL 674-1425

Fig. 8 Computed pattern for the f.c.c. lattice.

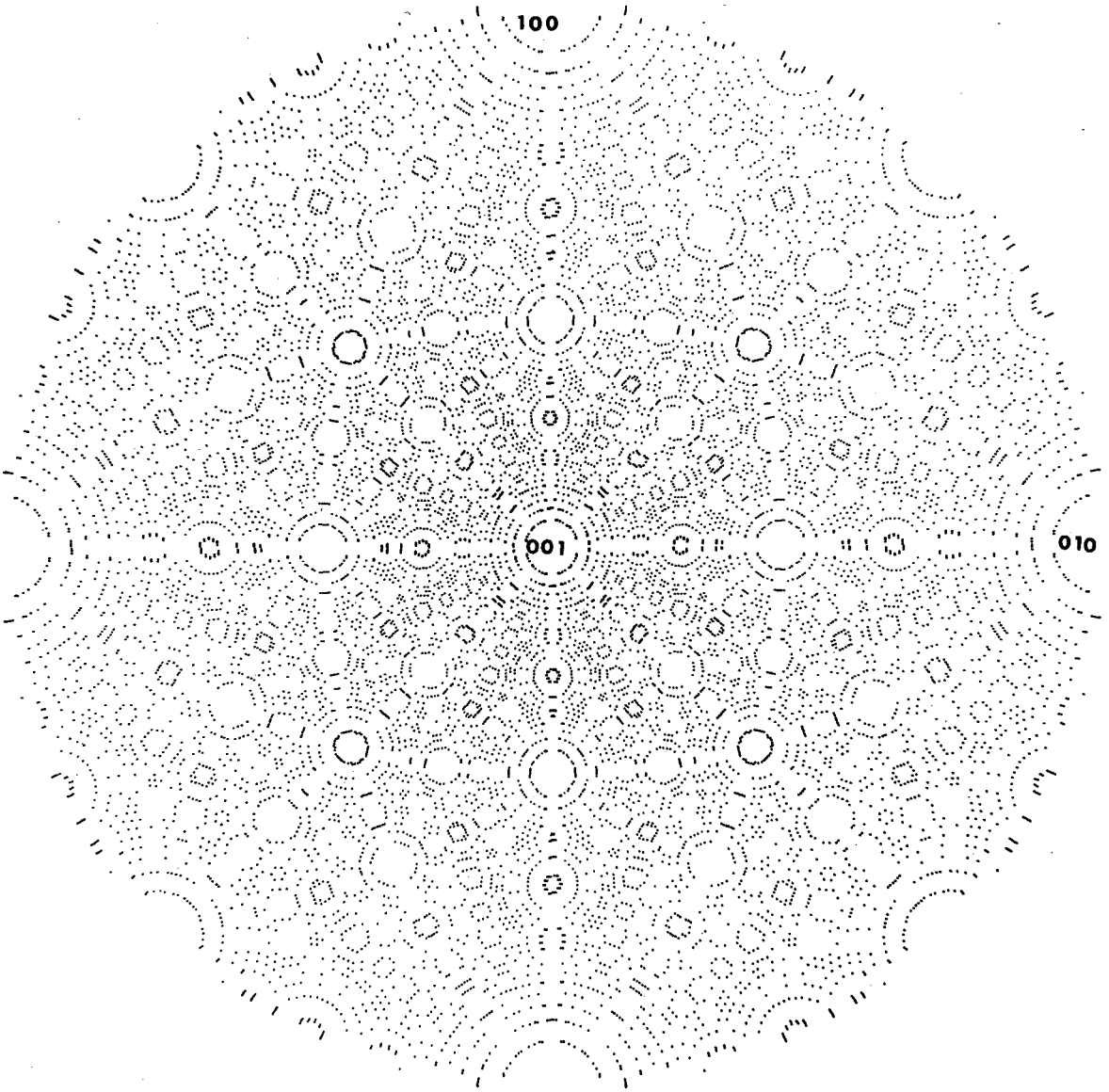

XBL 674-1426

Fig. 9 Stereogram for the simple cubic lattice. This was obtained from Fig. 5.

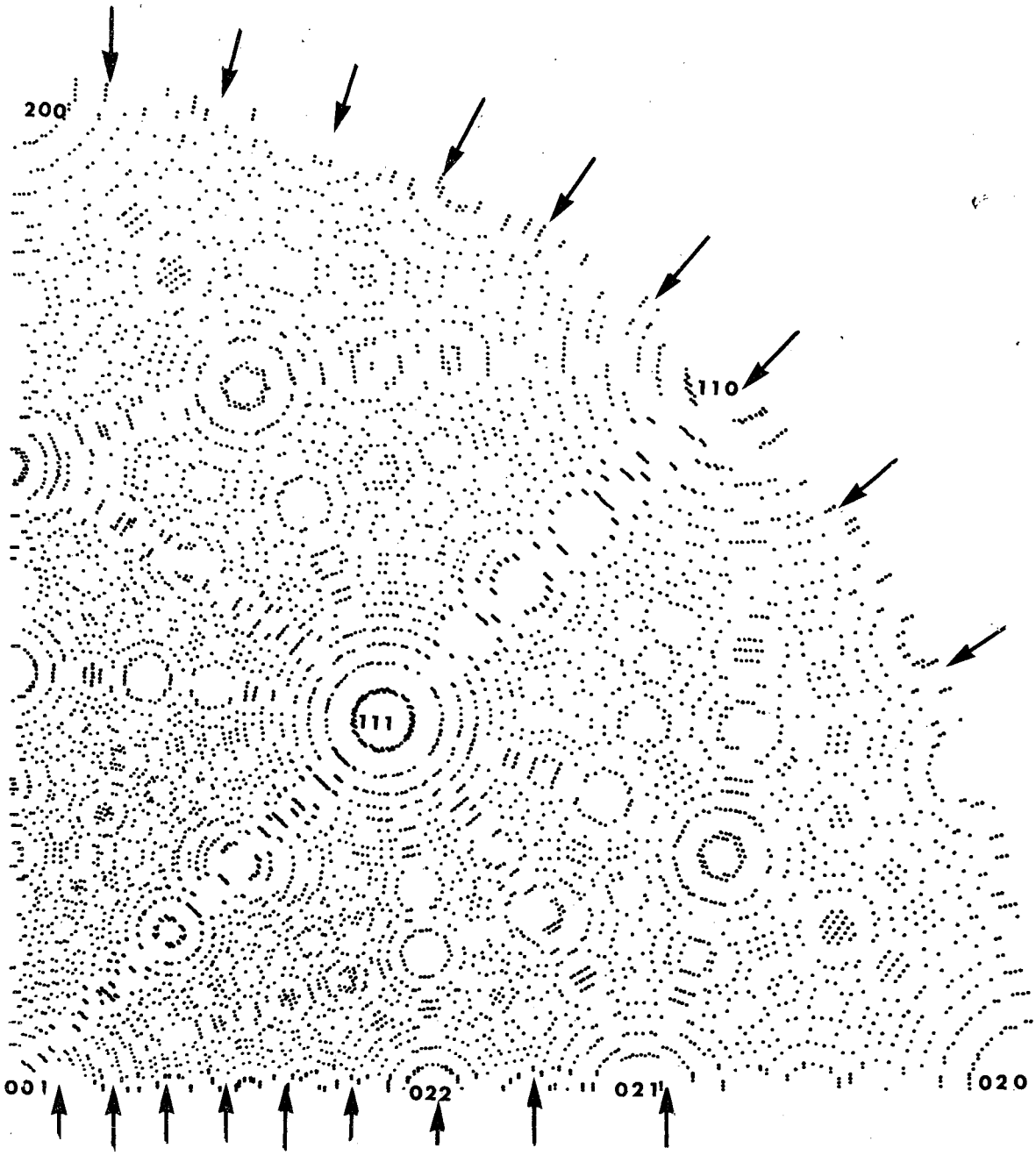

XBL 674-1427

Fig. 10 Periodic antiphase structure. This corresponds to CoPt II with cobalt atoms invisible. Every fourth antiphase boundary has been marked. The mismatch contrast can be seen on (001), (110), and (021) planes.

This report was prepared as an account of Government sponsored work. Neither the United States, nor the Commission, nor any person acting on behalf of the Commission:

A. Makes any warranty or representation, expressed or implied, with respect to the accuracy, completeness, or usefulness of the information contained in this report, or that the use of any information, apparatus, method, or process disclosed in this report may not infringe privately owned rights; or

B. Assumes any liabilities with respect to the use of, or for damages resulting from the use of any information, apparatus, method, or process disclosed in this report.

As used in the above, "person acting on behalf of the Commission" includes any employee or contractor of the Commission, or employee of such contractor, to the extent that such employee or contractor of the Commission, or employee of such contractor prepares, disseminates, or provides access to, any information pursuant to his employment or contract with the Commission, or his employment with such contractor.